Journal of Applied Polymer Science

Thermal processing influence on mechanical, thermal, and biodegradation behavior in poly(β-hydroxybutyrate)/poly(ε-caprolactone) blends: A descriptive model

Berenice Vergara-Porras,[1] Jorge Noel Gracida-Rodríguez,[2] Fermín Pérez-Guevara[3]

[1]Departamento de Biotecnología e Ingeniería Química, Escuela de Ingeniería y Ciencias. Tecnológico de Monterrey, Campus Estado de México, Carretera Lago de Guadalupe Km 3.5, Margarita Maza de Juárez. Atizapán de Zaragoza, Estado de México, México

[2]Biotecnología, Facultad de Química, Universidad Autónoma de Querétaro. Cerro de las campanas s/n, Las Campanas, Querétaro, Qro, México

[3]Departamento de Biotecnología y Bioingeniería, Centro de Investigación y de Estudios Avanzados (CINVESTAV), Avenida IPN 2508, Zacatenco. Gustavo a. Madero México D.F., México

Correspondence to: J. N. Gracida-Rodríguez (E-mail: gracidaj@netscape.net)

ABSTRACT: Poly(β-hydroxybutyrate) [PHB] is a biodegradable and biocompatible polymer produced by some bacteria genders. To improve mechanical properties, PHB has been blended with other polymers. Compression-molded blends of PHB and poly(ε-caprolactone) [PCL] (70/30 mass ratio) were cooled to room temperature following five different thermal treatments after molding at 180 °C. Blends processed with higher cooling rates were easier to biodegrade, nevertheless elongation at break and tensile strength decreased. Slower cooling kinetics and isothermal treatments increased perfection of crystals, as seen in differential scanning calorimetry and X-ray diffraction and spherulites size. A descriptive model is proposed herein where thermal, biodegradation, tensile properties, and crystal features were related to cooling kinetics applied. It is proposed that properties of 70/30 (PHB/PCL) blends can be predetermined by an adequate control of thermal conditions during processing. © 2016 Wiley Periodicals, Inc. J. Appl. Polym. Sci. **2016**, *133*, 43569.

KEYWORDS: biodegradable; blends; molding; phase behavior; properties and characterization

Received 27 November 2015; accepted 22 February 2016
DOI: 10.1002/app.43569

INTRODUCTION

In 2012, more than 99770 tons of municipal solid waste were generated per day only in Mexico (data obtained from INEGI/Government of Mexico).[1] According to the Environmental Protection Agency (EPA), petroleum-based polymers represent almost 13% (w/w) of all solid urban debris generated.[2] The use of petroleum-based polymers has been extensive mostly for packing and shipping in spite of low biodegradation rate and almost impossible mineralization of these materials.[3,4] Therefore, many authors have proposed replacing this kind of polymers with biodegradable biosynthetic polymers such as poly(hydroxyalkanoates) (PHAs).[5]

PHAs are polymers synthesized by a wide number of bacteria under stress conditions representing storage of carbon and energy. The most common PHA accumulated by bacteria is the homopolymer poly(β-hydroxybutyrate) [PHB].[4] Besides its biodegradability and biocompatibility, PHB application is limited due to its poor mechanical properties. Blending is a technique used for generating new materials with a variety of properties. Production of PHB blends, immiscible and miscible, has been extensively reported.[5]

Poly(ε-caprolactone) [PCL] is a polyester produced by the ring-opening polymerization of ε-caprolactone. PCL is reported also as biodegradable and biocompatible.[10–13] PCL has been blended with PHAs using the casting method.[13–16] The presence of two polymeric phases comes as a result from immiscibility of PHB and PCL in their blends.[6] Kumagai and Doi[7] reported the separation of macrophases in PHB and PCL blends thus affecting mechanical properties of blends. Gassner and Owen[8] confirmed phase separation in PHB/PCL blends finding that PCL in proportions higher than 60% produced a semicrystalline continuous PCL matrix in the blend and mechanical properties were dominated by PCL properties. In contrast, when PCL content is lower than 60%, PHB phase became the continuous phase and PCL inclusions did not affect blend rigidity. The presence of a two-phase system in solvent-casted blends of PHB and other PHB copolymers with PCL has been thoroughly studied.[9–13]

PHB has been previously used as a crystallization model; by introducing changes on cooling temperature, cooling rates, and isothermal crystallization, differences in crystal length, number of spherulites, and lamellae thickness were observed.[14–17] For pure PHB, the interband space and the average ratio of spherulites increased when the crystallization temperature was increased.[14,16] Using sudden crystallization kinetics, the nuclei formation was impeded as well as the molecular array for crystal formation meanwhile, by using isothermal conditions, spherulites were larger and the crystals size was more homogeneous.[5,18]

Conditions applied to polymer processing affect not only spherulites length and morphology but also mechanical and physical features. As an example, Bouquey *et al.*[19] demonstrated that different surface structures and phases arrays were obtained for the same proportion polystyrene poly(methyl methacrylate) melt-mixed blends. Thus, by modifying the stirring velocity during melt mixing, Alig *et al.*[20] reported that stirring velocity modified the size and shape of the dispersed phase for polypropylene and polyolefin samples. Particularly, for a polyethylene/polystyrene (10/90) blend, different morphology and phase arrays were observed by changing thermal conditions during melt-mixing blend production. Blends were produced using mechanical mixing and compression molding.[21] For PHAs blends, as examples, Chiu *et al.*[22] reported the differential assemblage in PHB/poly (ethylene oxide) blends. Qiu *et al.* studied PHBV/PCL[23] and PHBV/poly(butylene succinate)[24] crystallization observing differences in polymers array.

Moreover, crystallinity and surface structure affect biodegradation rate. Higher percentage of crystallinity results in lower biodegradation rates.[5] For this reason, it is probable that organized arrays of crystalline-amorphous areas as spherulites could favor degradation processes. As example, Abe *et al.*[25] found that erosion velocity was increased when lamellae thickness decreased. It has been reported that the union of PHB-depolymerase on crystalline chain produced disordered PHB chains that were easier to degrade.[26–28]

Both PHB and PCL were previously reported as biocompatible. New applications reported of both materials are as drug delivery systems as well as enhancing cell growth or support material for injuries. In the biomedical field, it is well known that materials properties including biodegradation kinetics have to be strictly controlled. As previously described, blend processing affects crystallinity, phase arrays, and spherulites characteristics. Meanwhile, biodegradation is a function of phase arrays and crystal properties. No reports were found where blends production conditions, crystallinity, mechanical properties, and biodegradation were related.

In this work, thermal processing was modified on a single proportion PHB/PCL blend. A descriptive model explaining of how thermal processing affects thermal, mechanical, crystalline, and biodegradation characteristics of PHB/PCL blends in the same proportion is proposed herein. It suggests that some characteristics of PHB/PCL blends can be previously established by controlling thermal production conditions.

EXPERIMENTAL

Materials

PHB (M_w = 430 KDa) as 5 mm nominal size granules was supplied by Goodfellow (#BU396311, England); PCL pellets (M_w = 48–90 KDa) were obtained from Fluka (#81277, USA).

Preparation of the Blends

PHB and PCL were blended in a 70/30 (PHB/PCL) mass ratio. Blends were melt processed at 180 °C during 10 min in a Plasticorder mixing chamber (Brabender, Germany). Polymers were first added at a 20 rpm velocity. Velocity was increased to 40 rpm when both polymers were in the mixing chamber. Torque was followed by stirring, and a constant torque value was achieved in all cases. Homogeneous blending was assured by a calorimetric analysis using DSC.

The obtained blends were compression molded on a laboratory Carver press (USA) to obtain plates of 10 cm × 10 cm × 1 mm. Molding conditions were set at a temperature of 180 °C and a pressure of 4.9 MPa during 10 min. After holding time, blends were cooled using five different thermal treatments before removal from the mold. Treatment A: from 180 to 4 °C in 1 min; treatment B: from 180 to 20 °C in 10 min; treatment C: from 180 to 20 °C in 120 min; treatment D: from 180 to 53 °C in 10 min and an isothermal crystallization of blend at 53 °C during 480 min; treatment E: from 180 to 120 °C in 1 min, and then an isothermal crystallization at 120 °C during 120 min and from 120 to 53 °C in 1 min for an isothermal crystallization at 53 °C during 120 min.

As controls, one sheet of pure PHB and one of pure PCL were used. Pure polymers, as received, were first placed in a mixing chamber following the same steps described above. Compression mold of pure polymers was carried out following the same conditions as those used for blends. Pure polymers sheets were cooled following blend treatment B.

Thermal properties, crystallinity, tensile properties, surface morphology, and biodegradation were evaluated for all blends and pure polymers.

Thermal Properties

Thermal properties of blends were estimated using differential scanning calorimetry. DSC was performed in a DSC 2920 (TA instruments, USA). Two heating scans for each sample were done in aluminum pans containing 10 mg of blends. First heating was done at 10 °C/min from −20 to 220 °C. Then, samples were cooled at 10 °C/min and reheated at 10 °C/min from −20 to 220 °C. In particular, the first heating scan is used to erase any prior thermal history of the sample. For analyzing effects of thermal history, the first scanning results were used.

Crystallinity was calculated form DSC curves obtained during first scan as follows [eq. (1)]:

$$X_{DSC} = \frac{\Delta H_m}{\omega \cdot \Delta H_m^\circ} \quad (1)$$

where ω is the weight fraction of the considered polymer (0.3 for PCL and 0.7 for PHB), ΔH_m is the melting enthalpy (J/g) as calculated from the fusion endotherm in the DSC thermogram

Table I. Melting Temperatures, Estimated Enthalpies, and Percentage of Crystallinity (X_C) for 70/30 (PHB/PCL) Blends Processed under Different Thermal Treatments, According to First Heating DSC Scan

Thermal treatment	Global cooling rate (°C/min)	T_m^{PHB} (°C)	ΔH_m^{PHB} (J/g)	T_m^{PCL} (°C)	ΔH_m^{PCL} (J/g)	T_c (°C)	ΔH_{cc} (J/g)	X_C (%)
A	176	59.54	27.93	166.62	39.32	81.08	2.105	47.5^{B}
B	16	60.52	33.05	168.32	40.96	83.64	3.155	$52.3^{A,B}$
C	1.3	59.24	29.48	163.03	50.94	-	-	56.5^{A}
D	Isothermal for PCL	61.94	20.36	158.92	39.12	-	-	41.8^{C}
E	Isothermal for PHB and PCL	60.06	−28.12	159.65	−38.78	-	-	47.3^{B}

T_m, melting temperature; ΔH_m, melting enthalpy; T_c, crystallization temperature; ΔH_{cc}, crystallization enthalpy; X_C, degree of crystallinity. ^{A,B} Superscripts were obtained by Tukey–Kramer statistical analysis. Different letters represent different significant values.

and ΔH_m° is the heat of fusion for completely crystallized PCL (139.5 J/g)[29] and PHB (146 J/g).[16]

X-ray Diffraction

Crystallinity measurements were done using X-ray diffraction performed with a D8 Advance, Bruker diffractometer (USA). Data were acquired at 30 kV and 16 mA at 4.5°/min scanning angle from 5 to 60°.

Tensile Properties

Tensile strength, Young's modulus, and extension to break were determined according ASTM D882-91 method using an Instron Universal Material Testing Machine (USA). Testing conditions were load area of 0.1 cm^2, grid separation of 5 cm, and extension rate of 5 mm/min. Two load cells were used: 10 N for blends and pure PCL, and 100 N for pure PHB. Data reported were the average of at least five measurements.

Surface Morphology

Surface of sheets was observed using a JSM-35C Scanning Electron Microscope (Jeol, Japan). Test specimens were previously treated with OsO_4, ethanol, and dried with CO_2 at the critical point in a Samdri-780A (Tousimis, USA). Specimens were covered with carbon and gold in a Desk II, Denton Vacuum (USA) and then observed.

Biodegradation Properties

Biodegradation was studied according to the ASTM G21-90 technique using only *Penicillium funiculosum* specimen for biodegradation. Along biodegradation, CO_2 production was measured in a Gas Chromatograph SRI 8610C as a result of polymer mineralization. Data provided in this work were correlated with initial amount of carbon (mM) in the samples. Data are reported as specific CO_2 production. Respirometric data were modeled using Gompertz equation[30] modified:

$$CO_2 = CO_{2,max} \cdot e^{-\lambda \cdot e^{-\mu_{max} \cdot t}} \quad (2)$$

where,

$CO_{2,max}$ [mM/mM]: maximal specific CO_2 production;

λ [d]: lag phase;

μ_{max} [d^{-1}]: maximal specific CO_2 production rate.

At days 30 and 60, SEM observations were made. Samples during biodegradation were observed in a JSM-6510LV Microscope (Jeol, Japan). Test specimens were previously treated as indicated in the section "Surface Morphology" and then observed.

Statistical Analysis

All obtained results were analyzed using JMP statistical software (SAS, USA). At least three different repetitions were done for each value. Significant differences were estimated according Tukey–Kramer analysis with a 0.05 α value. Statistical analyses are shown as superscripts. Different letters indicate different significance values.

RESULTS AND DISCUSSION

Preparation of Blends

Five sheets of PHB/PCL blends were produced modifying thermal treatment during the compressed molding processing. All blends reported were produced using a weight proportion of 70% of PHB and 30% of PCL.

Global cooling rates applied to thermal treatments are reported in Table I. In case of isothermal treatments, global cooling rates were not estimated. Treatment D was applied for promoting PCL crystallization while treatment E for promoting both polymers crystallization.

Thermal Characterization

First run obtained from DSC analysis was analyzed to elucidate the influence of processing on thermal properties of the blends. During first heating scan, differences in melting enthalpies and thermic transitions were observed (Figure 1 and Table I). Changes could be associated with thermal treatment of blends as a result of the existence of different types, sizes, and quantity of crystals.

For transition between 50 and 70 °C, which corresponds to PCL melting temperature, no differences were observed excluding for a slight decrease in melting enthalpy for treatment D blend (Figure 1 and Table I). Decreasing of melting enthalpy indicated an increase in perfection of PCL crystals. treatment D, as described above, was done for promoting PCL crystallization. Decrease in melting enthalpy, and consequently crystallinity, could be attributable to perfection of crystals. At 53 °C, PCL

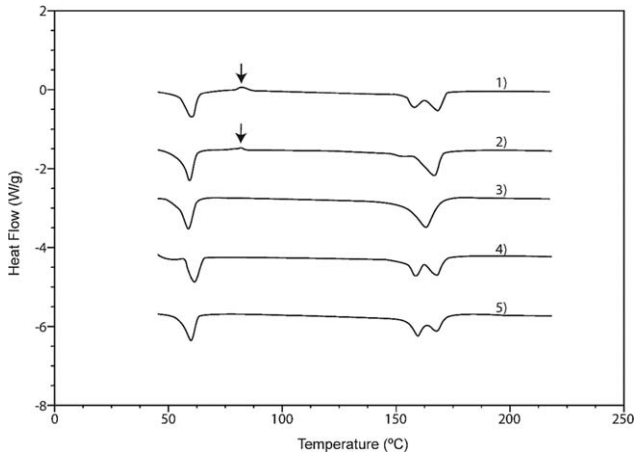

Figure 1. DSC thermograms of first run for 70/30 (PHB/PCL) obtained using the following crystallization kinetics: (1) treatment A, (2) treatment B, (3) treatment C, (4) treatment D, and (5) treatment E. Exothermic transitions are oriented in the positive *y*-axis.

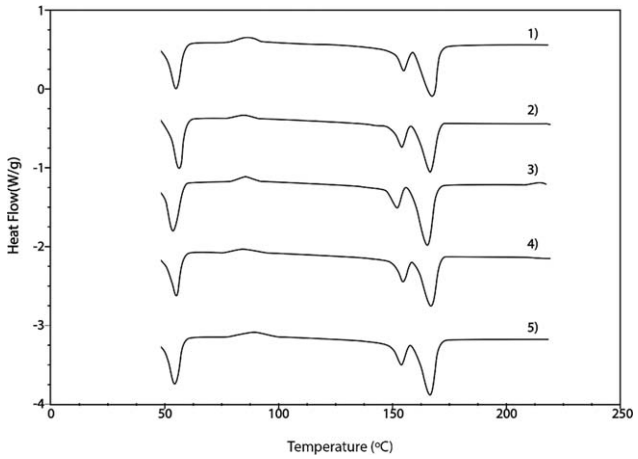

Figure 2. DSC thermograms of second run for 70/30 (PHB/PCL) obtained using the following crystallization kinetics: (1) treatment A, (2) treatment B, (3) treatment C, (4) treatment D, and (5) treatment E. Exothermic transitions are oriented in the positive *y*-axis.

crystals were allowed to growth slowly favoring correct molecules placing.

A second thermal transition was observed for only two blends as an exothermic crystallization signal (Figure 1, arrows). Those blends had the highest cooling rates: treatments A and B. Exothermal peaks have been reported for pure PHB associated with rapid crystallization processes. When cooling rate used was fast, adequate molecule accommodation was impeded; when energy was added, molecules vibrated, moved, and displaced to form crystals[31–34] giving an exothermic peak as a consequence of the process.

For PHB transition, observed in the range from 150 to 180 °C (Figure 1), differences in number and shape of peaks were observed. As an example, treatment A blend presented two melting peaks where the first is smaller than second one (Figure 1, line 1). This could be attributable to the cooling rate applied during processing. Sudden cooling could prevent crystal growth or crystallization nuclei formation could be impeded. The arrangement of few crystals formed could be impeding crystallization of other molecules. When energy was added during first scan of DSC, crystal formed could be melted and conditions became favorable for a second crystallization. Some molecules that were not able to crystallize during blend production could, in this second stage, form new crystals. As the temperature continues increasing, newly formed crystals remelt.

Treatment B presented also two melting peaks for PHB transition at 150–180 °C (Figure 1, line 2), being the first peak smaller. It is possible that few crystals were impeded to grow properly in that blend due to high cooling rate applied. In contrast, treatment C (Figure 1, line 3) blend presented one only melting peak indicating a more homogeneous crystal distribution. During slow cooling, molecules are allowed to place properly to create larger and more stable crystals. During first DSC heating, crystals previously formed melted in at one time. This behavior was previously reported by several authors and it is known as crystal perfection. More defined and sharper peaks show a higher degree of perfection and stability on crystals in contrast with wider transitions.[23,24,31,34–37]

Two melting peaks were also observed for treatment D. PHB crystallization was promoted at 120 °C for this treatment. Presence of multiple peaks for isothermal treatments has been reported previously. Hong and Chen[35] and Gunaratne and Shanks[32] reported that multiple melting peaks could be attributed to five different processes. However, for this work, due the conditions worked, multiple melting peaks could be related with (1) melting, recrystallization, and melting of newly formed crystal processes, (2) Polymorphism, different types of crystals, and (3) difference in crystals morphologies, i.e., differences in lamellae thicknesses and/or differences in distribution, perfection, and stability of crystals.

The degree of crystallinity of blends is essentially uniform, with an increase for treatment C (Table I). According to Abdelwahab *et al.*,[38] an increase in crystallinity is due to higher chain mobility and a better packing of segments. Low cooling rates could allow better packing of segments increasing crystal perfection.

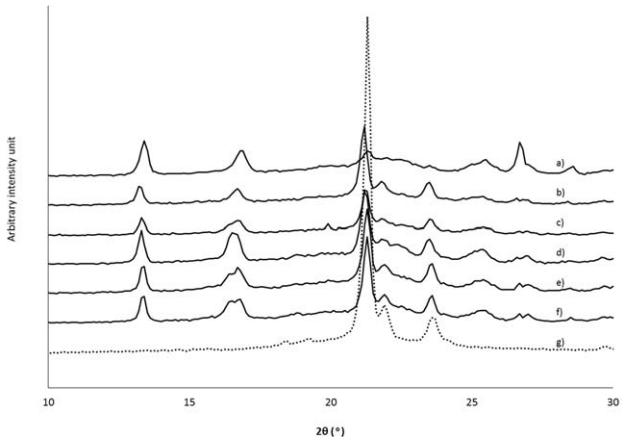

Figure 3. X-ray diffraction patterns of neat polymers and 70/30 (PHB/PCL) obtained using the following thermal treatments: (a) neat PHB, (b) treatment A, (c) treatment B, (d) treatment C, (e) treatment D, (f) treatment E, and (g) neat PCL.

Table II. Tensile Properties of 70/30 (PHB/PCL) Blends

Treatment	Elongation at break (%)	Tensile strength (MPa)	Young's modulus (MPa)
A	0.29 ± 0.51^{C}	0.5 ± 0.13^{B}	8.16 ± 0.8^{A}
B	ND	ND	ND
C	7.09 ± 0.64^{A}	1.43 ± 0.16^{A}	7.43 ± 0.6^{A}
D	$5.03 \pm 0.54^{A,B}$	1.43 ± 0.14^{A}	8.74 ± 0.63^{A}
E	$5.01 \pm 0.54^{A,B}$	1.39 ± 0.14^{A}	8.56 ± 0.59^{A}

^{A,B} Different superscript letters represent different significant values according to Tukey–Kramer statistical analysis.

It is possible also that interface interactions between PHB and PCL could influence nucleation of polymers. In addition, the decrease on melting enthalpies of blends processed with isothermal treatments may imply formation of a more stable structure. Isothermal treatments may increase movement of PCL molecules (in case treatment D) and PHB/PCL segments (in case treatment E) that facilitate subsequent crystallization. The decrease on crystallinity for treatment D may be also related with the increase of processing time (480 min at 53 °C) in comparison with treatment E (120 min at 53 °C).

When melting temperatures and transition enthalpies were estimated using second scan, no differences were found for any blend (Figure 2) confirming the same mass proportion in all cases.

X-ray Diffraction

PHB is a highly ordered polymer recognized to crystallize in an orthorhombic cell. The lattice parameters of PHB are $a = 0.576$ nm and $b = 1.32$ nm with a chain conformation in the left-handed 2_1 helix. Neat PHB analysis showed the presence of typical reflecting peaks at 2θ equals 13.4° and 16.8°, corresponding to the (020) and (110) planes and weak and broad peaks at 21.4°, 25.4°, 26.7°, and 28.6° corresponding, respectively, to the (021), (121), (040) and (002) planes as previously reported[38–40] (Figure 3, line a). Neat PCL displayed their main peaks at 2θ equal to 21.2°, 21.8°, and 23.5°, corresponding, respectively, to the characteristics (110), (111), and (200) reflection values typical of an orthorhombic crystalline unit cell as previously reported (Figure 3, line f).[6,41]

In general, patterns of PHB/PCL blends processed under different thermal conditions are very similar to neat PHB and neat PCL. Sharper peaks and higher peaks intensities were found at the (020) and (110) planes for PHB for treatment C indicating higher crystallinity and more stable crystal arrangements for PHB. A decrease in the intensity of typical reflecting peaks for PHB was observed for treatments A and B; peaks were wider in comparison with neat PHB and other blends.

Increase on intensity in peaks at 2θ equals 21° for treatments A, D, and E was observed; however, coincidence of reflective patterns of PHB and PCL allows no conclusion. Treatments D and E presented a more defined and sharper peaks at the (111) and (200) plane for PCL as an effect of isothermal crystallization. XRD results are in concordance with the thermal characterization of blends by DSC described previously.

Tensile Properties

Tensile properties were determined for all blends and pure polymers except for blend B. Macrofractures in the surface of treatment B blend impeded the adequate testing according the ASTM technique.

By analyzing tensile properties, no differences were found on Young's modulus for all blends referring that stiffness remains the same (Table II). The absence of significant differences in this value could be related to the presence of continuous layers from one out of the two materials, which form the blend. However, the arrangement of these layers depends on thermal treatment applied. This process is to be explained ahead.

Elongation at break and tensile strength were lower for treatment A blend (Table II). Elongation at break for treatment A blend was reduced more than 90% as long as tensile strength was 30% diminished when compared with other blends.

PHB brittleness has been related with its high crystallinity.[5,42] It was also shown previously that fast cooling rates impeded crystal formation. However, tensile properties estimated showed that mechanical properties are better in blends with low cooling rates (Table II). Herein, in this work, we proposed that these differences were related with differences in polymer accommodation attributed to thermal treatments used during blend molding as explained ahead.

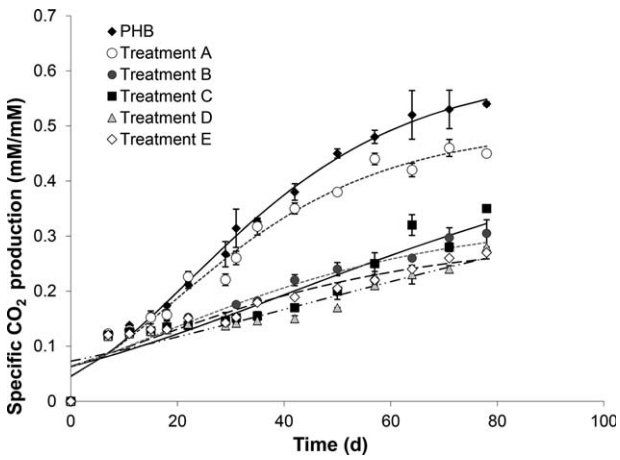

Figure 4. Specific CO_2 production during PHB and 70/30 (PHB/PCL) blends biodegradation. CO_2 production was related with the initial carbon contained in sample (mM/mM).

Table III. Gompertz Parameters Calculated during Biodegradation with *P. funiculosum*

Treatment	$CO_{2,max}$ (mM/mM)	μ_{max} (d^{-1})	Λ (d)
Pure PHB	0.6 ± 0.05^{A}	0.042 ± 0.002^{A}	2.5 ± 0.47^{A}
A	$0.5 \pm 0.03^{A,B}$	0.044 ± 0.003^{A}	2.38 ± 0.15^{A}
B	$0.53 \pm 0.05^{A,B}$	$0.031 \pm 0.0015^{A,B}$	1.68 ± 0.5^{A}
C	$0.34 \pm 0.08^{B,C}$	$0.19 \pm 0.002^{B,C}$	2.13 ± 0.45^{A}
D	$0.47 \pm 0.07^{B,C}$	$0.014 \pm 0.001^{B,C}$	1.87 ± 0.35^{A}
E	0.29 ± 0.08^{C}	$0.016 \pm 0.003^{B,C}$	1.54 ± 0.05^{A}

Different superscript letters represent different significant values according to Tukey–Kramer statistical analysis.

Biodegradation Kinetics

Carbon dioxide production, as a result of mineralization of blend, was measured during 90 days. Carbon dioxide production kinetic is shown in Figure 4. Evidence of changes in easiness of mineralization of blends was found.

In enzymatic studies, it has been described that enzymes responsible for biodegradation of polymers contain three domains: a binding domain, an active site, and a linker domain.[5,26,43,44] Binding domain attaches preferentially to crystalline zone, whereas the active site hydrolyzes preferably the amorphous material. Monomers obtained from polymer hydrolysis (R-3-hydroxybutyric acid from PHB and ε-caprolactone from PCL) are water-soluble and pass through cell membrane, where they are metabolized by β-oxidation and tricarboxylic acid cycle. Under aerobic conditions, polymers are converted into CO_2 and water.[45] The mass balance equation for aerobic biodegradation polymers is given in eq. (3).[46]

$$C_T = C_R + CO_2 + C_B \quad (3)$$

Where C_T is the total carbon, C_R is any residue of the polymer that is left, CO_2 is the carbon dioxide produced, and C_B is the biomass produced by microorganism through reproduction and growth.

Carbon dioxide production was modeled using the Gompertz equation [eq. (2)]. Maximal specific CO_2 production rate (μ_{max}), lambda (λ), and maximal CO_2 production are shown in Table III. The lag phase represented with lambda was similar in all cases. Meanwhile, μ_{max} estimated with the Gompertz equation was higher for PHB and treatment A blend. This μ_{max} parameter referred to the easiness of the substrate to be

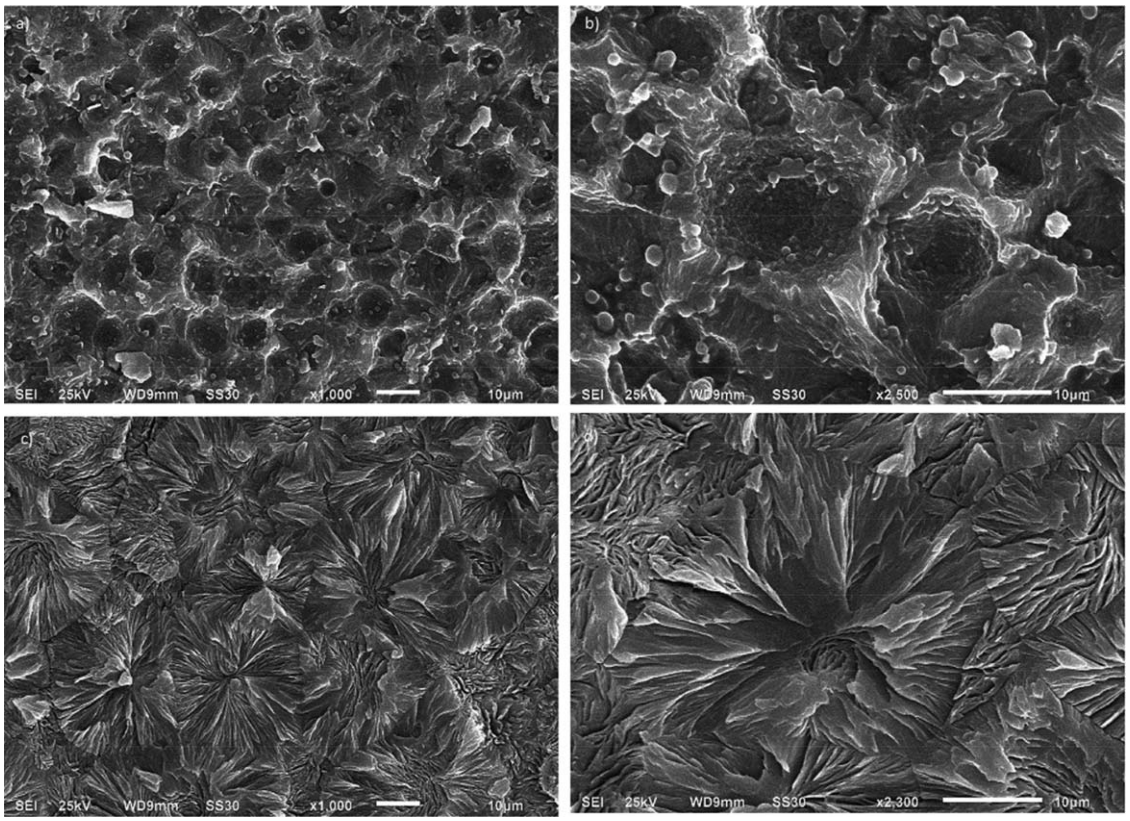

Figure 5. Spherulites observed on (a,b) pure PHB and (c,d) pure PCL on surface after 60 days of biodegradation using *P. funiculosum*.

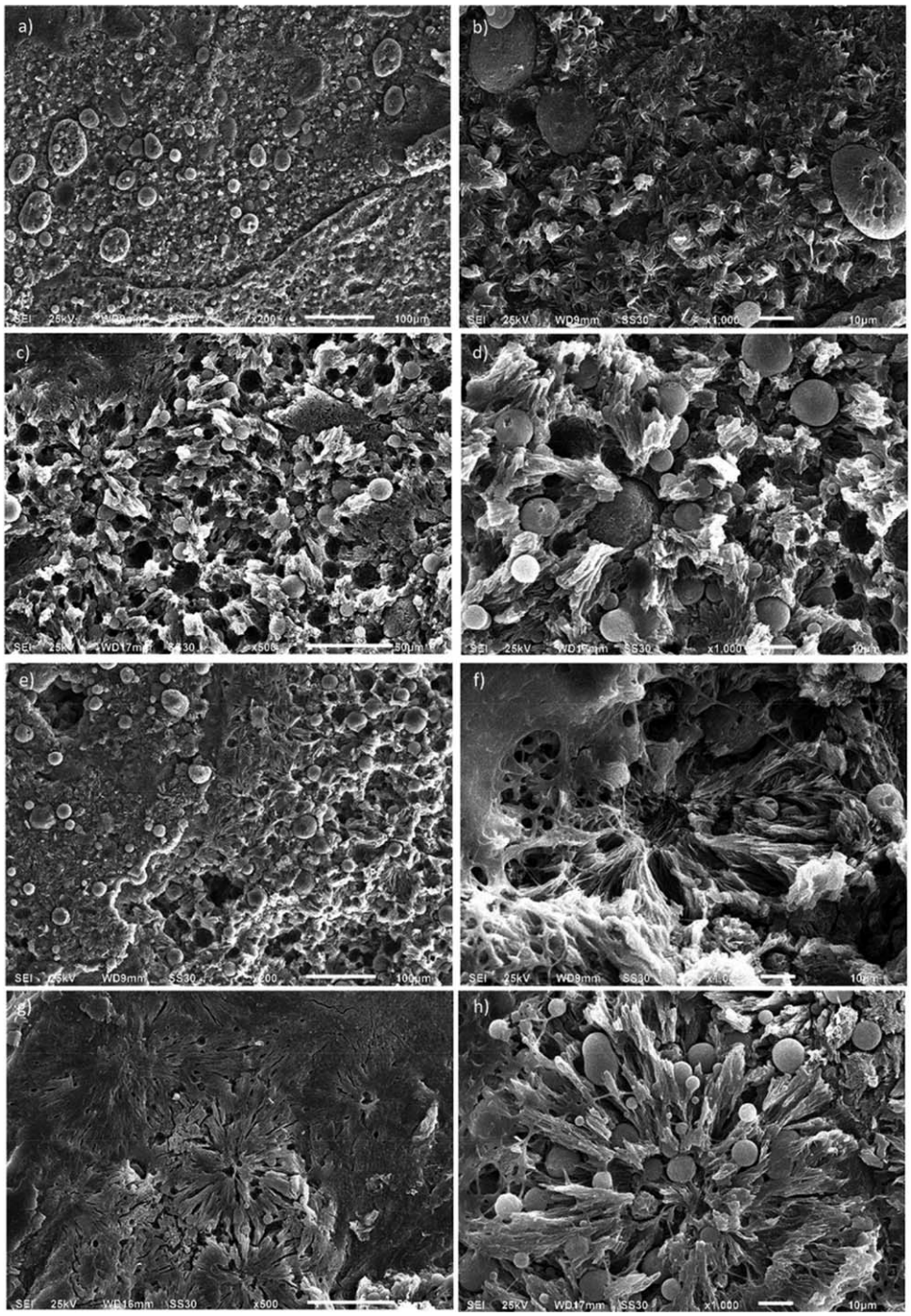

Figure 6. Typical spherulite morphology observed after 60 days of biodegradation on the surface of 70/30 (PHB/PCL) under different thermal treatments: (a,b) treatment A; (c,d) treatment B; (e,f) treatment C; (g,h) treatment D.

degraded. The results obtained for CO_{2max} indicated that blends processed with treatments D and E were not completely mineralizable.

Treatment A blend presented a rate of biodegradation similar to pure PHB. This could be attributable to two different characteristics. According to Barham *et al.*[15,16] for pure PHB, fast cooling rates produce smaller disordered crystal structures. Kumagai *et al.*[7] described that when a PHB depolymerase of *Alcaligenes faecalis* was used, enzymatic hydrolysis was reduced by increasing PHB crystallinity. Differences in biodegradation rates could be a result of the size and types of crystals, as determined previously in first heating DSC scan. As an example, for treatment A blend, the presence of smaller crystals and the slight increase of amorphous phase could favor blend degradation.

On the other hand, polymer arrangement could also favor the degradation of some blends. If PHB was placed preferentially on

Table IV. Typical Crystal Arrangements Size Observed in 70/30 (PHB/PCL) Blends Produced Using Different Thermal Treatments

Treatment	Crystal size (μm)
Pure PHB	16.3 ± 2.3^{C}
Pure PCL	35 ± 5^{C}
A	8 ± 2.1^{C}
B	ND
C	15 ± 3^{C} 120 ± 10^{A}
D	78 ± 8.5^{B}
E	ND

^{A,B,C} Different superscript letters represent different significant values according to Tukey–Kramer statistical analysis.

surface, blend degradation rate could be increased. For *Penicillium* sp., PHB is more easily to assimilate than PCL.[47] Results indicated than for pure PCL, less than a 10% of biodegradation was achieved applying only *P. funiculosum* for degradation after 60 days.[11] Therefore, presence of PHB in surface could favor the hydrolytic enzymes secretion increasing degradation of PCL in the blend. This effect could explain the increased degradation rate obtained for blend A.

The maximal specific CO_2 production ($CO_{2,max}$) could also be related with production thermal processing applied to blends. Isothermal crystallization (treatments D and E) increased the amount, size, and perfection of crystals of PCL (at 53 °C) and PHB (at 120 °C). It was possible that the lower values of $CO_{2,max}$ obtained for those blends were an indication of the existence of crystalline areas, impossible to access or degrade by *P. funiculosum*.

Even PHB depolymerase of *P. funiculosum* had been reported previously as specific for PHB degradation[12]; $CO_{2,max}$ parameter indicated that PCL was also degraded. Lovera *et al.*[13] found that, for a PHB/PCL blend, polymers are attacked in synergy due to components dispersion. Gonçalves and Martins-Franchetti[10] found that PCL degradation is exclusively of amorphous phase. In contrast, Abe *et al.*[25] reported the enzymatic hydrolysis of crystalline phase in the edges of PHB chains. The cuts in the lamellae edges increase mobility through the crystal resulting in disordered PHB chains easier to hydrolyze by enzymes. All those reports support the idea of PCL being degraded favored by the presence of PHB. It was possible that presence of PHB enhance excretion of depolymerases, lipases, and hydrolases by *P. funiculosum*. Once enzymes were excreted, PHB was preferentially degraded but some molecules of PCL could also be degraded. This effect could be enhanced for blends produced with the higher cooling rates.

After 60 days of biodegradation, regular crystalline structures were observed. Spherulites and crystal arrangements were present in all blends and in pure polymers as shown in Figures 5 and 6. For pure polymers, significant differences on crystal geometry were observed (Figure 5). For PHB, spherulites were observed [Figure 5(a,b)]. Lamellae structures were degraded beginning by the center of crystals. For pure PCL, no evidence of crystal degradation was observed [Figure 5(c,d)]. It seemed that surface-amorphous phase was the only substrate that *P. funiculosum* could hydrolyze.

For the blends, differences in sizes and number of spherulites were observed. As it can be seen in Figure 6 and Table IV, spherulite size was lower when higher cooling rates were applied. Isothermal treatments allowed crystallization of blends, and higher sizes of spherulites. Spherulites sizes, as well as crystallinity, could affect also biodegradation.

Results presented herein are in concordance with previously published reports. For blends, Gonçalves and Martins-Franchetti[10] reported that for PHBV/PCL blends microorganisms attacked terminal edges of PHBV chains, while PCL was hydrolyzed on amorphous zone. Degradation induced changes on PCL domains adjacent to PHBV domains. For PHB/PCL blend, Kumagai and Doi[7] observed that enzymatic hydrolysis was favored in some proportions using PHB depolymerase of *Alcaligenes faecalis* T1 due morphological changes of PHB in PCL matrix. Lovera *et al.*[13] using *A. flavus* for degradation of PHB/PCL found that PCL was hydrolyzed on surface; due phase segregation, depolymerase was diffused trough the solvent-casted blend, affecting PCL. All authors coincided that phase dispersion generated larger surface areas.

In Figure 7, transversal cuts of blends are shown. Differences of mycelial penetration were observed. It was also observed that surface of the blends with lower cooling rates is rich in PCL. In transversal cuts for suddenly crystallized blend, mycelia penetrates deeper—more than 200 μm [Figure 7(c,d)]. It seems that *P. funiculosum* grew first on surface and then, mycelia penetrated the surface to degrade PHB located in the center of the blend. Crystallization kinetics could also modify polymer placing. Different placing of polymers in the blend could also affect the manner than *P. funiculosum* grew and the degradation kinetics. For treatments B and C, *P. funiculosum* growth was more superficial. Even, no evidence of penetration was observed for treatment C blend [Figure 7(g,h)]. For pure PHB, no penetration of mycelia was observed however; *P. funiculosum* growth was prolific, covering all surface in a thick monocape.

Both PHB and PCL are highly crystalline polymers that form spherulites while crystallizing.[7,14,34,37] From the melt, spherulites are typically obtained as crystalline arrangements with regular symmetry starting from a nucleation center. Spherulites crystals are arranged as lamellas and within the interlamellar spaces, the polymer in amorphous phase is present.[14,48] Spherulites morphology and crystallinity depend on crystallization conditions, i.e., the thermal conditions applied during processing of polymers.

Proposed Model

Figure 8 shows the model describing the arrangement of polymers during low cooling rates as in treatment C. In the beginning, both polymers are in liquid phase at a temperature of 180 °C under 4.9 MPa of pressure [Figure 8(a)]. Both polymers are mixed sharing the space without any molecular interaction. When temperature starts to decrease, nucleation centers are

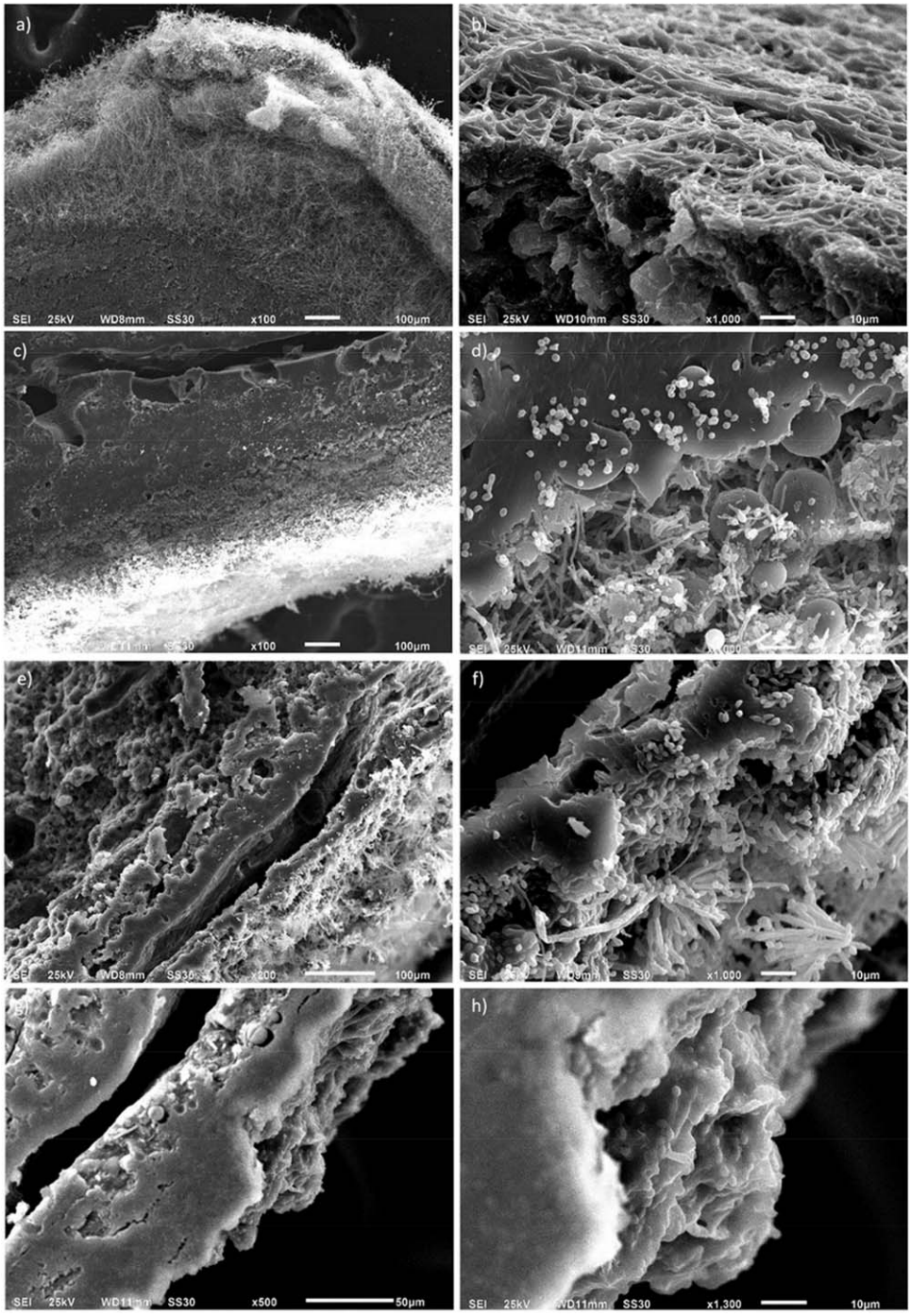

Figure 7. Transversal cut after 30 days of biodegradation on 70/30 blend using different thermal production: (a,b) PHB; (c,d) treatment A; (e,f) treatment B, and (g,h) treatment C.

formed. Newly formed PHB crystals start to branch and separate in different directions forming PHB spherulites. Amorphous PHB is placed within the interlamellar space. At this point, PCL continues in liquid state [Figure 8(b)]. As temperature continues decreasing gradually, PHB spherulites are placed at one located area forming a continuous phase [Figure 8(c)]. When temperature is close to 60 °C, PCL also forms crystals. PCL crystallization is completed over a continuous PHB phase [Figure 8(d)]. The blend is then formed with two separated phases. As the phases formed are continuous, resultant yield stress and breakage resistance are higher.

When isothermal crystallization is applied, crystals and spherulites are allowed to grow (Figure 9). Isothermal treatments imply the formation of more stable and packaged structures. Spherulites are larger, and crystal perfection increases. Hence, results obtained for blends processed with treatments D and E are explained.

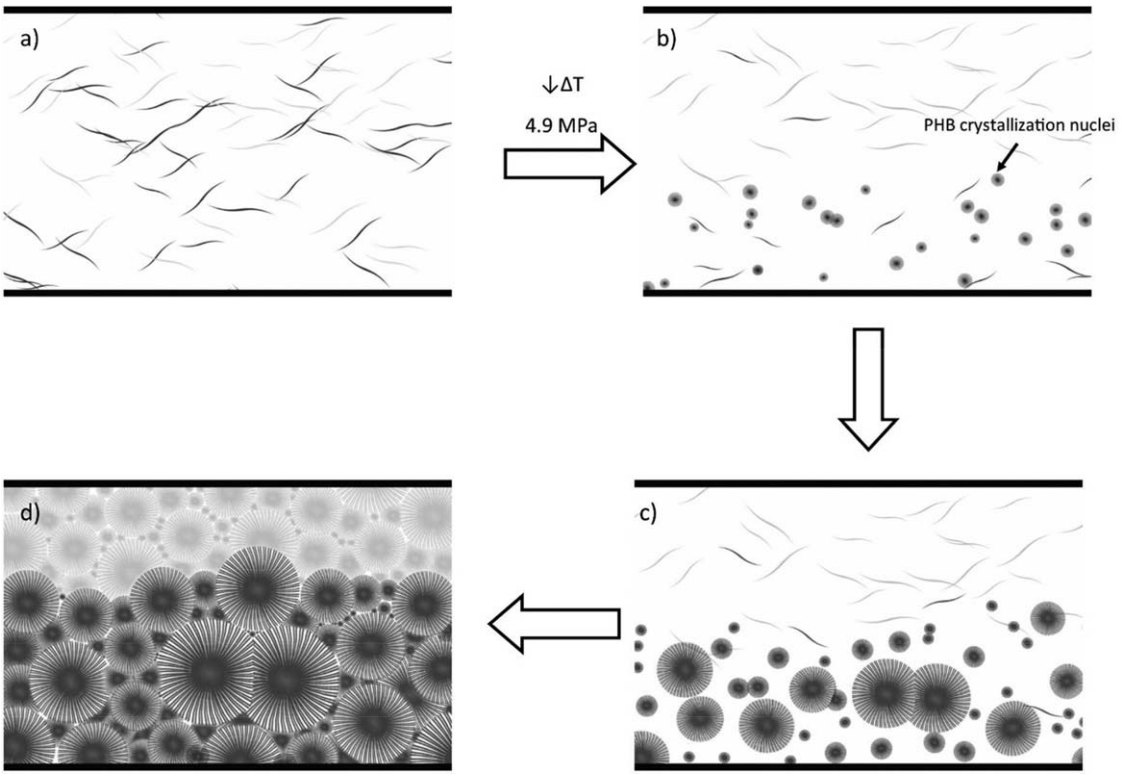

Figure 8. Proposed model of solidification of PHB/PCL blends at lower $\Delta H/t$ rates, i.e., slow decreases on temperature. PHB was schematized on blue color while orange was used for PCL representation. Figure is only for model depicting; crystal sizes are not proportional on image.

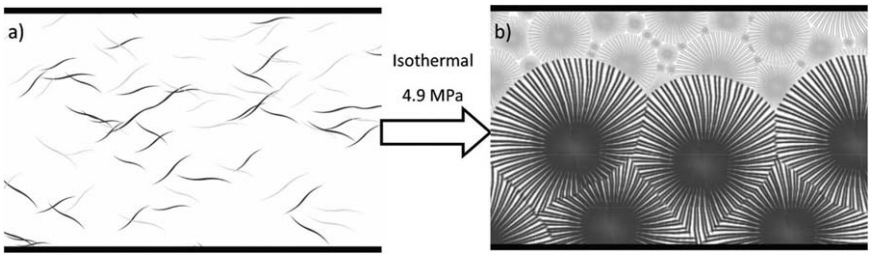

Figure 9. Proposed model of solidification of PHB/PCL blends applying isothermal crystallization. PHB was schematized on blue color while orange was used for PCL representation. Figure is only for model depicting; crystal sizes are not proportional on image.

When cooling rates applied were higher—as in treatment A and B—quicker changes on temperature may have allowed simultaneous crystallization of both polymers (Figure 10). Although no miscibility was observed, PHB molecules remained inside PCL crystals and PCL molecules inside PHB crystals. It may be possible that a weak interaction in physical space did occur. Therefore, phases were discontinuous which turned blends brittle.

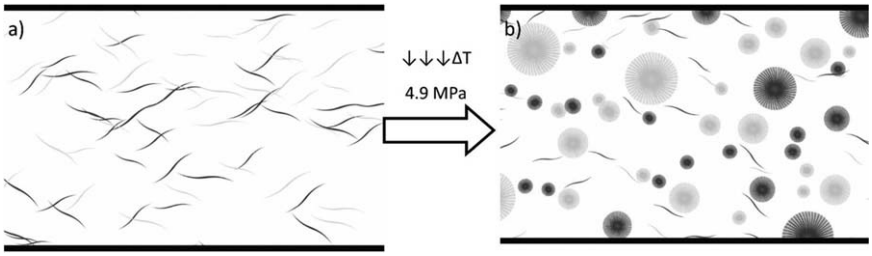

Figure 10. Proposed model of solidification of PHB/PCL blends at higher $\Delta H/t$ rates i.e., sudden cooling rates. PHB was schematized on blue color while orange was used for PCL representation. Figure is only for model depicting; crystal sizes are not proportional on image.

CONCLUSIONS

Thermal treatment influenced mechanical and thermal properties, as well as, biodegradation kinetics of 70/30 (PHB/PCL) blends processed under different thermal conditions. Differences in biodegradation rates and mechanical properties were attributed to differences in polymers accommodation in blends and differences on crystalline structure. A descriptive model was proposed, where crystal, thermal, and degradation properties were related with thermal processing of blends.

Spherulites were observed by SEM after removal of *P. funiculosum* at day 60 of biodegradation. Isothermal cooling kinetics increased crystals size. Slow cooling produced crystals with heterogeneous sizes; meanwhile, rapid and sudden cooling kinetics impeded adequate crystal formation.

It is proposed that by controlling thermal production kinetics of the blends, biodegradation kinetics, thermal and mechanical properties, and crystallinity could also be controlled.

ACKNOWLEDGMENTS

This work was carried out at CINVESTAV. Vergara-Porras received grant-aided support from CONACyT (No. 203514). Authors strongly appreciate Manuel Cervantes-Uc, Alejandro May-Pat (Material Department, CICY), Alberto Tecante (UNAM), and Humberto Vázquez-Torres (UAM-I) for technical support during blend preparation and characterization. Support of the Microscopy Section of CINVESTAV, particularly Sirenia González aid during microscopy images acquisition was invaluable. Images were kindly designed by I. Vergara-Porras. Manuscript recommendations of R. Espadas-Zita and J. Corona-Hernández are honestly and greatly acknowledged.

REFERENCES

1. Municipal Solid Waste Generation, Recycling and Disposal in the United States: Non-Hazardous Waste, Municipal Solid Waste for 2013; U.S. Environmental Protection Agency (EPA), Washington, DC, 2013; http://www3.epa.gov/epawaste/nonhaz/municipal/.
2. Censo Nacional de Gobiernos Municipales y Delegacionales, **2013**. Módulo 6. Residuos Sólidos Urbanos; Instituto Nacional de Estadística y Geografía (INEGI), Ciudad de México, México, 2012; http://www.beta.inegi.org.mx/
3. Arrieta, M. P.; Samper, M. D.; Lopez, J.; Jimenez, A. *J. Polym. Environ.* **2014**, *22*, 460.
4. Gasser, E.; Ballmann, P.; Droege, S.; Bohn, J.; Koenig, H. *J. Appl. Microbiol.* **2014**, *117*, 1035.
5. Ha, C. S.; Cho, W. J. *Progr. Polym. Sci.* **2002**, *27*, 759.
6. Del Gaudio, C.; Ercolani, E.; Nanni, F.; Bianco, A. *Mater. Sci. Eng. A* **2011**, *528*, 1764.
7. Kumagai, Y.; Doi, Y. *Polym. Degrad. Stab.* **1992**, *36*, 241.
8. Gassner, F.; Owen, A. J. *Polymer* **1994**, *35*, 2233.
9. Antunes, M. C. M.; Felisberti, M. I. *Polímeros: Ciência e Tecnologia* **2005**, *15*, 134.
10. Goncalves, S. P. C.; Martins-Franchetti, S. M. *J. Polym. Environ.* **2010**, *18*, 714.
11. Vergara-Porras, B.; Gracida-Rodriguez, J.N.; Perez-Guevara, F. *J. Polym. Environ.* **2011**, *19*, 834.
12. Jenkins, M. J.; Cao, Y.; Howell, L.; Leeke, G. A. *Polymer* **2007**, *48*, 6304.
13. Lovera, D.; Marquez, L.; Balsamo, V.; Taddei, A.; Castelli, C.; Muller, A. J. *Macromol. Chem. Phys.* **2007**, *208*, 924.
14. Ding, G.; Liu, J. *Colloids Polym. Sci.* **2013**, *291*, 1547.
15. Barham, P. J. *J. Mater. Sci.* **1984**, *19*, 3826.
16. Barham, P. J.; Keller, A.; Otun, E. L.; Holmes, P. A. *J. Mater. Sci.* **1984**, *19*, 2781.
17. Righetti, M. C.; Di Lorenzo, M. L. *Thermochim. Acta* **2011**, *512*, 59.
18. Birley, C.; Briddon, J.; Sykes, K. E.; Barker, P. A.; Organ, S. J.; Barham, P. J. *J. Mater. Sci.* **1995**, *30*, 633.
19. Bouquey, M.; Loux, C.; Muller, R.; Bouchet, G. *J. Appl. Polym. Sci.* **2011**, *119*, 482.
20. Alig, I.; Steinhoff, B.; Lellinger, D. *Measurement Sci. Technol.* **2010**, 21.
21. Ling, G. H.; Shaw, M. T. *Polymer* **2009**, *50*, 4917.
22. Jiang-Wen, Y.; Hsiu-Jung, C.; Trong-Ming, D. *Polymer* **2003**, *44*, 4355.
23. Qiu, Z. B.; Yang, W. T.; Ikehara, T.; Nishi, T. *Polymer* **2005**, *46*, 11814.
24. Qiu, Z. B.; Ikehara, T.; Nishi, T. *Polymer* **2003**, *44*, 7519.
25. Abe, H.; Doi, Y.; Aoki, H.; Akehata, T. *Macromolecules* **1998**, *31*, 1791.
26. Murase, T.; Suzuki, Y.; Doi, Y.; Iwata, T. *Biomacromolecules* **2002**, *3*, 312.
27. Numata, K.; Kikkawa, Y.; Tsuge, T.; Iwata, T.; Doi, Y.; Abe, H. *Biomacromolecules* **2005**, *6*, 2008.
28. Numata, K.; Hirota, T.; Kikkawa, Y.; Tsuge, T.; Iwata, T.; Abe, H.; Doi, Y. *Biomacromolecules* **2004**, *5*, 2186.
29. Pitt, C. G.; Chasalow, F. I.; Hibionada, Y. M.; Klimas, D. M.; Schindler, A. *J. Appl. Polym. Sci.* **1981**, 3779. p
30. Zwietering, M. H.; Jongenburger, I.; Rombouts, F. M.; Vantriet, K. *Appl. Environ. Microbiol.* **1990**, *56*, 1875.
31. Gunaratne, L.; Shanks, R. A.; Amarasinghe, G. *Thermochim. Acta* **2004**, *423*, 127.
32. Gunaratne, L.; Shanks, R. A. *Thermochim. Acta* **2005**, *430*, 183.
33. Gunaratne, L.; Shanks, R. A. *Eur. Polym. J.* **2005**, *41*, 2980.
34. Gunaratne, L.; Shanks, R. A. *J. Therm. Anal. Calorim.* **2006**, *83*, 313.
35. Hong, S.-G.; Chen, W.-M. *e-Polymers* **2006**, *44*, 310.
36. Hong, S. G.; Hsu, H. W.; Ye, M. T. *J. Therm. Anal. Calorim.* **2013**, *111*, 1243.
37. Gunaratne, L.; Shanks, R. A. *J. Polym. Sci. B: Polym. Phys.* **2006**, *44*, 70.
38. Abdelwahab, M. A.; Flynn, A.; Chiou, B. S.; Imam, S.; Orts, W.; Chiellini, E. *Polym. Degrad. Stabil.* **2012**, *97*, 1822.

39. Owen, A. J.; Heinzel, J.; Skrbic, Z.; Divjakovic, V. *Polymer* **1992**, *33*, 1563.
40. Bruckner, S.; Meille, S. V.; Malpezzi, L.; Cesaro, A.; Navarini, L.; Tombolini, R. *Macromolecules* **1988**, *21*, 967.
41. Lovinger, A. J.; Han, B. J.; Padden, F. J.; Mirau, P. A. *J. Polym. Sci. B: Polym. Phys.* **1993**, *31*, 115.
42. D'Amico, D. A.; Cyras, V. P.; Manfredi, L. B. *Thermochim. Acta* **2014**, *594*, 80.
43. Yamashita, K.; Aoyagi, Y.; Abe, H.; Doi, Y. *Biomacromolecules* **2001**, *2*, 25.
44. Hisano, T.; Kasuya, K. I.; Tezuka, Y.; Ishii, N.; Kobayashi, T.; Shiraki, M.; Oroudjev, E.; Hansma, H.; Iwata, T.; Doi, Y.; Saito, T.; Miki, K. *J. Mol. Biol.* **2006**, *356*, 993.
45. Shah, A. A.; Hasan, F.; Hameed, A.; Ahmed, S. *Biotechnol. Adv.* **2008**, *26*, 246.
46. Jayasekara, R.; Harding, I.; Bowater, I.; Lonergan, G. *J. Polym. Environ.* **2005**, *13*, 231.
47. Pandey, J. K.; Reddy, K. R.; Kumar, A. P.; Singh, R. P. *Polym. Degrad. Stabil.* **2005**, *88*, 234.
48. Abo El Maaty, M. I. *Polymer* **2002**, *43*, 6535.